0.33 m at the fault. Continuation of the 1897 datum by means of the 1902 survey data indicates that uplift between 1897 and 1914, averaging about 0.3 m, may have persisted northward as far as Mojave. Comparisons between the results of the 1914 and 1926 San Pedro to Mojave surveys suggest that the 1897/1902–1914 uplift had partially collapsed by 1926 by amounts that increased more or less uniformly northward to a maximum of 0.38 m immediately south of the San Andreas and averaged about 0.3 m northward across the western Mojave block. The interval between the apparently aseismic 1897/1902–1914 uplift and this seeming collapse is not known to have been associated with any significant seismic event other than the 1916 "Tejon Pass" earthquake, which was characterized by a relatively small seismic moment (*6*). Nevertheless, the 1897/1902–1914 uplift differed significantly from that developed during the 1959–74 interval in that it was much more clearly associated with the Transverse Ranges, and specifically the frontal fault system, than it was with the San Andreas. Moreover, although we may never be able to demonstrate the point conclusively, circumstantial evidence argues that the 1897/1902–1914 uplift was confined largely and perhaps exclusively to the Transverse Ranges, and that as much as 0.3 m of the uplift that occurred within the northern Transverse Ranges and the western Mojave block is probably specious and attributable simply to systematic error in the 1914 leveling.

Whether or not the described upift (Fig. 1) will continue to enlarge both laterally and vertically is problematic. A comparison with the seismicity of this region since 1932, and especially since 1960 (*7*), shows that the area elevated above 0.15 m has remained virtually free of seismic activity west of the 117th meridian (except for the area north of Lebec, which has continued to experience aftershock activity associated with the 1952 Kern County earthquakes); this correlation between uplift and seismic quiescence is particularly striking if the comparison is restricted to earthquakes of magnitude 4 or larger. Hence, if it is assumed (i) that this uplift (Fig. 1) is either a direct or an indirect effect of elastic strain accumulation; (ii) that any future seismic activity will coincide roughly with the pattern of activity after 1932; and (iii) that the presumably continuing seismic activity east, south, and north of the uplifted area is a significant index of elastic strain release, any future lateral growth may be restricted to the northwest, an area in which we lack appropriate geodetic control. Parenthetically, the southeast end of the uplifted area, near Cajon, coincides closely with the southeastern extent of reported surface rupturing associated with the great 1857 earthquake on the San Andreas; the uplifted zone extends northwestward along the San Andreas at least two-thirds the length of the 1857 zone of surface breakage, which was traced as far as Cholame (*8*).

Continued monitoring of the uplifted area is desirable not only to assess further growth of this feature, but to detect any reversals in movement as well. For example, comparisons between geodetic data developed within the epicentral region both before and immediately after the 1971 San Fernando earthquake suggest a tilt reversal north of the epicenter that may have preceded the main shock (*2*). However, regardless of its desirability, detailed monitoring of this vast area by means of frequently repeated level surveys seems prohibitively costly. Alternatively, precise gravity surveys with a resolution of ± 6 to 9 μgal (equivalent to a free-air difference of 2 to 3 cm) are now considered feasible (*9*); combining these surveys with perhaps biannual releveling across the short axis of the uplifted area, so that each could be continually checked against the other, might provide a relatively inexpensive yet highly reliable monitoring system.

ROBERT O. CASTLE
JACK P. CHURCH
MICHAEL R. ELLIOTT

U.S. Geological Survey,
345 Middlefield Road,
Menlo Park, California 94025

References and Notes

1. S. D. Hicks, *Shore Beach* **40** (No. 1), 23 (1972).
2. R. O. Castle *et al.*, *Geology* **2**, 61 (1974).
3. This 0.05-m figure is probably unrealistically large. The south half of the combined 1959/60 leveling (Fig. 2) was carried out during the period April–May 1960; the north half was surveyed during the interval March–April 1959. If any positive movements occurred along the south half of this line between 1959 and 1960, they would diminish the magnitude of any uplift after March–April 1959 based on a comparison between the combined 1959/60 datum and the results of any later leveling along the full length of the line.
4. J. M. Buchanan-Banks, R. O. Castle, J. I. Ziony, *Tectonophysics*, in press.
5. R. O. Castle, J. P. Church, M. R. Elliott, N. L. Morrison, *ibid.*, in press.
6. T. C. Hanks, J. A. Hileman, W. R. Thatcher, *Geol. Soc. Am. Bull.* **86**, 1131 (1975).
7. J. A. Hileman, C. R. Allen, J. M. Nordquist, *Seismicity of the Southern California Region, 1 January 1932 to 31 December 1972* (Seismological Laboratory, California Institute of Technology, Pasadena, 1973), pp. 55–64.
8. C. W. Jennings (compiler), *Calif. Div. Mines Geol. Prelim. Rep. 13* (1973).
9. H. W. Oliver, personal communication.
10. Prepared in cooperation with the National Geodetic Survey. We thank R. A. Page, J. C. Savage, and W. R. Thatcher for suggestions and comments.

26 January 1976

Diamonds in an Upper Mantle Peridotite Nodule from Kimberlite in Southern Wyoming

Abstract. *Diamonds in a serpentinized garnet peridotite nodule from a diatreme in southern Wyoming are the first known occurrence in an upper mantle peridotite xenolith from a kimberlite intrusion in North America as well as the second authenticated occurrence of diamonds from kimberlite pipes in North America. The nodule is believed to have come from a section of depleted (partially melted) lherzolite at a depth of 130 to 180 kilometers.*

Small diamond crystals have been recognized in an altered garnet peridotite nodule from a kimberlite diatreme in southern Wyoming. This is one of a very few reported occurrences of diamond in a peridotite xenolith from a kimberlite intrusion. Dawson and Smith (*1*) have identified diamond in a mica-garnet lherzolite from the Mothae kimberlite in northern Lesotho. Sobolev *et al.* (*2*) have found diamonds in five nodules of garnet serpentinite (altered garnet peridotite) from the Aykhal kimberlite diatreme in Siberia. The Wyoming discovery is only the second authenticated occurrence of diamonds from a kimberlite locality in North America; the other occurrence was in the Murfreesboro district of Pike County, Arkansas, where diamonds were first found in 1906 and were recovered commercially until 1919 (*3*).

The presence of diamond in the Wyoming nodule was first suspected when F. J. Nowacki and R. Jensen encountered difficulties in preparing thin sections at the U.S. Geological Survey in Denver, Colorado. They noticed deep scratches on a grinding plate and isolated a small white crystal (approximately 1 mm in diameter) as the source of the problem. X-ray diffraction analysis by T. Botinelly and B. F. Leonard (U.S. Geological Survey), using a Gandolfi camera, confirmed the diamond identification. Subsequent examination of the nodule revealed that three small diamonds were embedded in the rock, and additional small crystals were isolated when parts of the nodule were dissolved in hydrofluoric acid.

The diamonds range in diameter from 0.1 to 1.0 mm except for one crystal cleaved along a (111) plane, which is approximately 1.0 by 1.5 mm on that surface. Although some of the crystals have rounded and hackly surfaces with only minor face development (or preservation), most crystals show at least some well-developed octahedral faces. These faces commonly are composed of superimposed lamellae of progressively smaller sizes that produce a pronounced stepped or terraced appearance (Fig. 1A). One crystal (approximately 0.2 mm) embedded in the surface of the nodule is a near-perfect octahedron, except for weakly developed, narrow, striated dodecahedral faces that probably formed by incipient lamellar buildup of octahedral faces (Fig. 1, B and C). Reentrant angles on some crystals infer twinning, which appears to be controlled by both (111) and interpenetrant twin laws. The coloration of the diamonds ranges from white to colorless and grayish black. The grayish black diamonds have surficial ridges of graphite along dodecahedral face striations; there are also graphite platelets within the crystals, probably an alteration along cleavage planes.

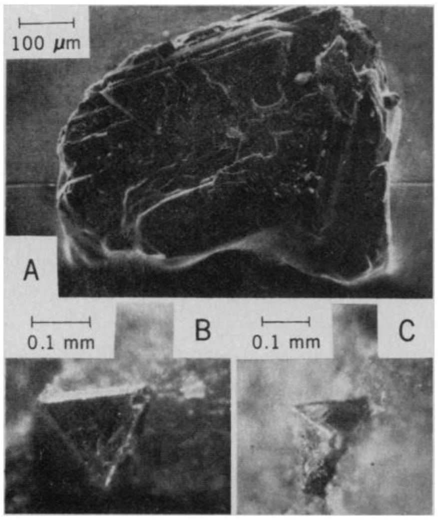

Fig. 1. Photographs of diamond crystals from serpentinized garnet lherzolite nodule 1117. (A) Scanning electron micrograph of lamellar buildup on octahedral faces. (B) Diad view of a simple octahedral diamond crystal showing weak development of narrow dodecahedral faces by incipient lamellar growth on (111) faces. (C) Tetrad view of the same diamond crystal.

The diamond-bearing nodule (sample 1117) is rounded and oblate and has the dimensions 9 by 11.5 by 12.5 cm. Although it has been intensely serpentinized and silicified, the original tabular texture [terminology of Bouiller and Nicolas (*4*)] is well preserved. Also present are narrow zones, interpreted to be zones of shear, which have a porphyroclastic to mosaic texture and which parallel the long dimensions of the nodule.

Despite the alteration, the original mineralogy of the nodule can also be recognized. Olivine and orthopyroxene, although completely serpentinized and replaced locally by carbonate and quartz, can be recognized by grain outlines and by differences in serpentine fabric, the bastite after orthopyroxene reflecting pyroxene cleavage. Pseudomorphs after olivine and orthopyroxene are as long as 0.5 cm. Clinopyroxene (chrome diopside) is also completely replaced by serpentine, talc, and quartz, but the pseudomorphed grains retain a characteristic green color as opposed to the yellow brown and pale brown of the altered olivine and orthopyroxene. Clinopyroxene (completely altered) is quite subordinate to olivine and orthopyroxene (less than 10 percent of the rock); it is concentrated mainly in the zones of shear as recrystallized aggregates in stringers and porphyroclasts. Unaltered primary minerals include garnet and the minor accessory chromite. The chromite is believed to be primary because unaltered nodules contain similar crystals (Table 1). The garnet occurs as rounded crystals that are as much as 3 mm in diameter; the chromite is generally highly irregular in shape and occupies interstitial sites. Also present are numerous small, irregular grains of Cu-Zn alloy and Ni metal as large as 1 mm in diameter.

The diamond-bearing nodule is one of several hundred xenoliths collected from a group of kimberlite diatremes in southern Wyoming and northern Colorado that have been studied intermittently for several years (*5*, *6*) and are tentatively established as Late Silurian or Early Devonian. These xenoliths, most of which are less altered than sample 1117, have been considered to be inclusions of upper mantle material in the enclosing kimberlite (*6*) and have been used to construct a model of the upper mantle based on the chemistry of the coexisting minerals of the xenoliths (Fig. 2). Probably long before kimberlite eruption, the mantle from the base of the crust (approximately 50 km at present) to a depth of at least 180 km consisted of spinel and garnet lherzolite, which through epi-

Table 1. Chemical analyses of minerals from garnet lherzolite nodules. We carried out the analyses by electron microprobe, using methods described by Finger and Hadidiacos (*17*).

Oxide concentration	Sample number* and mineral								
	1117, garnet	1117, spinel	1040, clinopyroxene	1040, garnet	S2L102, clinopyroxene	S2L102, garnet	S2L102, orthopyroxene	S2L102, olivine	S2L102, spinel
SiO_2	40.8	0.32	55.3	41.2	54.7	41.5	57.4	41.0	0.14
TiO_2	0.09	0.30	0.26	0.6	0.07	0.16	0.04	0.00	0.8
Al_2O_3	14.3	7.5	2.0	17.4	1.9	19.5	0.7	0.02	11.8
Cr_2O_3	12.3	61.1	2.3	7.4	2.0	5.1	0.30	0.00	55.3
Fe_2O_3		3.7							3.1
FeO	6.0	11.3	2.6	6.5	2.3	7.2	4.8	8.1	14.6
MnO	0.38	0.27	0.11	0.38	0.12	0.36	0.13	0.12	0.31
MgO	21.4	14.2	18.0	20.6	17.3	20.7	35.8	50.7	12.6
NiO	0.00	0.07	0.01	0.00	0.05	0.00	0.06	0.35	0.00
CaO	4.7	0.01	18.1	5.7	19.7	5.2	0.53	0.04	0.00
Na_2O	0.03	0.04	1.73	0.05	1.7	0.05	0.07	0.00	0.00
K_2O	0.00	0.00	0.01	0.00	0.00	0.00	0.00	0.00	0.00
Totals	100.00	98.81	100.42	99.83	99.84	99.77	99.83	100.33	98.65

*Sample descriptions: sample 1117, serpentinized diamond-bearing garnet peridotite nodule from Wyoming kimberlite pipe; sample 1040, serpentinized garnet peridotite nodule (with unaltered clinopyroxene) from Wyoming kimberlite pipe; sample S2L102, unaltered garnet peridotite nodule from the Sloan 2 kimberlite pipe, Colorado.

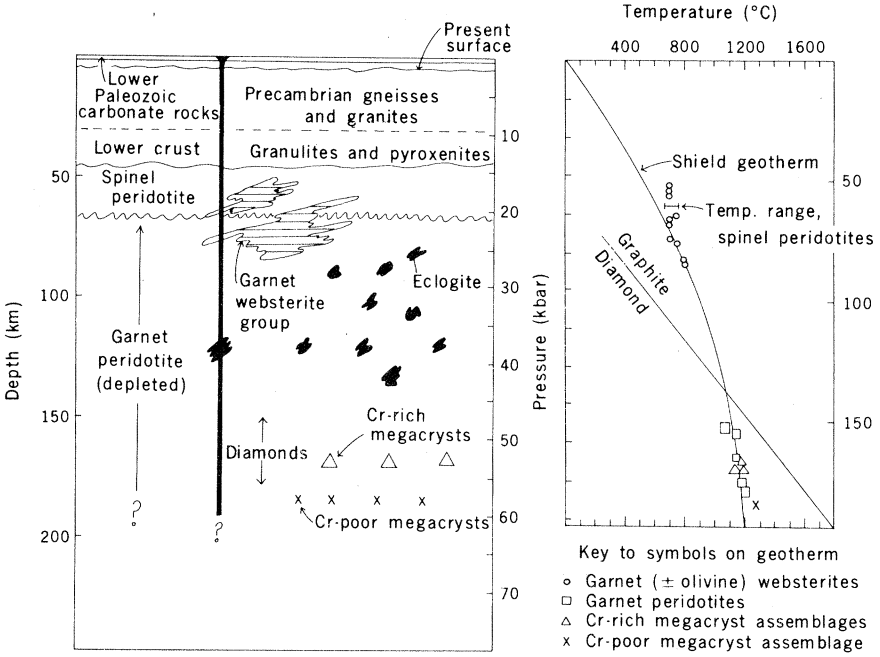

Fig. 2. Schematic model of the crust and mantle beneath the Front Range of Colorado and Wyoming in Devonian time, reconstructed from nodules in kimberlite pipes, and the inferred temperature distribution with depth. The shield geotherm was independently computed (*13*); equilibration temperatures and pressures plotted for particular nodules were calculated in this study.

sodes of partial melting was depleted of less refractory elements and enriched in more refractory elements, such as Mg and Cr (*7*). The Cr_2O_3 contents of the garnets are 4 to 15 percent (by weight) and of the diopsides are 1.0 to 2.5 percent. The Mg/(Mg + Fe) (atomic) ratios of the olivines are 0.90 to 0.93 and of the diopsides are 0.91 to 0.95. A group of large (> 1 cm) monomineralic megacrysts of diopside, orthopyroxene, and garnet (the Cr-rich megacrysts, Fig. 2) have compositions similar to those of minerals of depleted lherzolites.

On the basis of the abundance of unaltered nodules, partially or completely altered nodules (like nodule 1117), and grains from disaggregated nodules (*6*), spinel or garnet lherzolite is believed to have been the principal upper mantle material, although other material was also present. Eclogite nodules are believed to have come from pockets within peridotite (*6*); they are interesting for their chemical heterogeneity (*6*) and for a variable accessory assemblage, including kyanite, corundum, ilmenite, rutile, sphene, and orthoclase. A group of garnet clinopyroxenites, garnet websterites, and garnet olivine websterites (websterite group) contains minerals that have a Mg/(Mg + Fe) content similar to that of depleted lherzolites but are relatively low in Cr_2O_3 content. Clinopyroxenes have a higher content of Na_2O (*6*). A few peridotite nodules from one pipe contain lenses consisting of garnet and pyroxenes having mineral chemistries similar to that of websterite. From this evidence, websterites are believed to have formed lenses within peridotite. Another major nodule group is Cr-poor megacrysts of orthopyroxene, subcalcic diopside, garnet, and ilmenite; this group is very similar to a megacryst group found in the Lesotho pipes (*7*). Lamellar intergrowths of subcalcic diopside and magnesian ilmenite have been found in nearby kimberlite pipes at Iron Mountain, Wyoming (*8*).

Equilibration temperatures and pressures of nodules containing two pyroxenes and garnet (with or without olivine) are displayed in Fig. 2 [see (*9, 10*) for method of calculation]. Although the positions of these points can be changed by different data reduction or thermometric-barometric grids (*11, 12*), both the garnet websterite group points and the garnet lherzolite (plus megacrysts) points fall near an independently derived shield geotherm (*13*). From spinel peridotites and eclogites, only equilibration temperatures can be obtained (*9, 10*). On the assumption (*14*) that spinel peridotites and eclogites have equilibrated along the same geotherm, spinel peridotites are confined to depths of less than 65 km and eclogites to depths of 75 to 130 km.

The textures of the peridotite nodules are variable. Unlike the model for the Lesotho nodules of Boyd (*11*), for these nodules there appears to be little correlation of deformation texture with depth. Porphyroclastic textures appear in nodules of the spinel peridotite and websterite groups from 60 to 90 km, although the bulk of these nodules have granular textures. All the depleted garnet peridotite nodules that are sufficiently unaltered to permit an analysis of requisite minerals plot in a restricted depth range (150 to 180 km); yet those nodules have textures ranging from granular to tabular to porphyroclastic to, in a few samples, mosaic and fluidal mosaic (*4*).

Although not all phases of the diamondiferous nodule 1117 have been preserved, there is little doubt from petrographic examination (see above) and electron microprobe analyses of garnet and chromite (Table 1) that the nodule was a depleted garnet lherzolite. All oxide concentrations of the garnet fall within the ranges established for garnet lherzolites from these pipes (*6*). The equilibration conditions of the nodule cannot, of course, be calculated. However, other peridotite nodules having Cr-rich garnet from the same pipe have clinopyroxene preserved (but no olivine or orthopyroxene). They give temperatures of 1050° to 1150°C, for which equilibration depths along the geotherm (Fig. 2) are 130 to 180 km; an example is nodule 1040 (Table 1). Moreover, an unaltered lherzolite nodule (sample S2L102) from the Sloan 2 pipe, about 20 km to the south, contains garnet similar to that in samples 1117 and 1040. Its garnet is not as Cr-rich as the garnet in sample 1117, but the nodule contains more chromite. Calculated equilibration conditions for sample S2L102 are 1060°C and 48 kbar. Thus, by analogy, the diamondiferous nodule 1117 may have equilibrated at 1050° to 1150°C and 40 to 55 kbar (a depth of 130 to 180 km).

The major phases of sample S2L102 (Table 1) are remarkably similar chemically to those of diamond-bearing mica-garnet lherzolite nodule BD2125, described by Dawson and Smith (*1*), for which equilibration conditions of 1050°C and about 46 kbar were calculated (42 kbar by the method used here). Garnet of nodule BD2125 contains 5.5 percent Cr_2O_3 as compared with 5.1 percent for sample S2L102. The MgO and CaO contents of garnets in peridotites S2L102, 1117, and BD2125 are also similar. Garnets in the Aykhal diamondiferous serpentinites contain 4.9 to 14.1 percent Cr_2O_3 and 1.9 to 6.2 percent CaO (*15*); 1.9 percent CaO is comparable to the CaO content of some garnet inclusions in diamond (*2, 16*).

On the basis of available chemical data, it would appear that all known diamondiferous peridotites have come from depleted sections of the upper mantle. As yet unanswered are the questions of whether the diamonds grew in the presence of melt during that depletion process and what relation such diamonds bear to the great majority of diamonds in kimberlite.

M. E. McCallum
Department of Earth Resources,
Colorado State University,
Fort Collins 80523, and
U.S. Geological Survey,
Box 25046, Denver Federal Center,
Denver, Colorado 80225

David H. Eggler
Geophysical Laboratory,
Carnegie Institution of Washington,
Washington, D.C. 20008

References and Notes

1. J. B. Dawson and J. V. Smith, *Nature (London)* **254**, 580 (1975).
2. V. S. Sobolev, B. S. Nai, N. V. Sobolev, Yu. G. Laurent'ev, L. N. Pospelova, *Dokl. Acad. Sci. USSR Earth Sci. Sect.* **188**, 168 (1969).
3. H. D. Miser and C. S. Ross, *Bull. U.S. Geol. Surv.* **735**, 279 (1922).
4. A. M. Bouiller and A. Nicolas, *Phys. Chem. Earth* **9**, 467 (1975).
5. J. Chronic, M. E. McCallum, C. S. Ferris, Jr., D. H. Eggler, *Geol. Soc. Am. Bull.* **80**, 149 (1969); D. H. Eggler and M. E. McCallum, *Carnegie Inst. Washington Yearb.* **72**, 446 (1973); M. E. McCallum, *Contrib. Geol.* **13**, 17 (1974); ———— and D. H. Eggler, *Am. Mineral.* **56**, 1735 (1971); ————, L. K. Burns, in *Extended Abstracts, International Conference on Kimberlites,* L. H. Ahrens, A. R. Duncan, A. J. Erlank, Eds. (University of Cape Town, Rondebosh, Cape Town, South Africa, 1973), p. 217; *Phys. Chem. Earth* **9**, 149 (1975).
6. D. H. Eggler and M. E. McCallum, *Carnegie Inst. Washington Yearb.* **73**, 294 (1974).
7. F. R. Boyd and P. H. Nixon, in *Lesotho Kimberlites*, P. H. Nixon, Ed. (Lesotho National Development Corporation, Maseru, 1973), p. 48.
8. M. E. McCallum, C. B. Smith, L. K. Burns, D. H. Eggler, W. A. Braddock, *Geol. Soc. Am. Abstr. Programs* **7**, 628 (1975).
9. Equilibration temperatures are obtained from the Ca/(Ca + Mg) content of diopside coexisting with orthopyroxene and the experimentally determined $CaMgSi_2O_6$-$MgSiO_3$ solvus. For spinel peridotites, websterites, and olivine websterites the solvus of D. H. Lindsley and S. A. Dixon [*Geol. Soc. Am. Abstr. Programs* **7**, 1171 (1975)] was used, giving lower temperatures than the solvus of B. T. C. Davis and F. R. Boyd [*J. Geophys. Res.* **71**, 3567 (1966)]. However, the spinel peridotite temperatures are in accord with temperatures derived from the Al_2O_3 content of orthopyroxene coexisting with spinel and olivine (*10*). For garnet lherzolites and megacrysts (with inclusions of other phases of the megacryst group) either the Lindsley-Dixon solvus or the Davis-Boyd solvus yields similar results. Eclogite temperatures were obtained from clinopyroxene-garnet Fe-Mg partitioning [K_D (partitioning coefficient)] data at a pressure of 30 kbar [A. Råheim and D. H. Green, *Contrib. Mineral. Petrol.* **48**, 179 (1974)]. Temperatures range from 800° to 1025°C. Equilibration pressures were obtained from the Al_2O_3 content of orthopyroxene coexisting with garnet and clinopyroxene by the method of B. J. Wood [*Contrib. Mineral. Petrol.* **46**, 1 (1974)], with the exception that Wood's term for the Cr content of garnet was not used. That term appears to overcorrect pressure for Cr-rich garnets. Pressures were not calculated for spinel peridotites inasmuch as the Al_2O_3 content of orthopyroxene is essentially independent of pressure (*10*).
10. M. Obata, in *International Conference on Geothermometry and Geobarometry, Extended Abstracts* (Pennsylvania State Univ. Press, University Park, 1975).

→ F. R. Boyd, *Geochim. Cosmochim. Acta* **37**, 2533 (1973).

12. G. M. Brown, *Nature (London)* **255**, 671 (1975).
13. S. P. Clark and A. E. Ringwood, *Rev. Geophys.* **2**, 35 (1964).
14. F. R. Boyd [*Carnegie Inst. Washington Yearb.* **73**, 285 (1974)] deduced from nodules at the Frank Smith Mine that spinel peridotites recorded temperatures higher than the geotherm. Spinel peridotites in Wyoming kimberlites, however, record suitably low temperatures (< 900°C), and there is no geologic evidence in this region of an igneous or metamorphic event during the Paleozoic era that could have heated rocks to temperatures greater than the ambient geotherm.
15. N. V. Sobolev, *The Deep-Seated Inclusions in Kimberlites and the Problem of the Upper Mantle Composition* (Nauka, Siberian Branch, Novosibirsk, 1974) (American translation: American Geophysical Union, Washington, D.C., in press).
16. H. O. A. Meyer and F. R. Boyd, *Geochim. Cosmochim. Acta* **36**, 1255 (1972).
17. L. W. Finger and C. G. Hadidiacos, *Carnegie Inst. Washington Yearb.* **71**, 598 (1972).
18. We thank J. W. Adams, R. L. Parker, F. R. Boyd, B. O. Mysen, I. Kushiro, D. Smith, and H. S. Yoder, Jr., for their helpful comments on the manuscript. Research supported by the Earth Sciences Section, National Science Foundation, NSF grant DES 74-13098, and by the Carnegie Institution of Washington. Publication authorized by the director, U.S. Geological Survey.

28 January 1976

A Novel Means for Dealing with L-Canavanine, a Toxic Metabolite

Abstract. *L-Canavanine is a highly toxic L-arginine analog found in some leguminous seeds. Larvae of the bruchid beetle* Caryedes brasiliensis, *collected in Costa Rica, subsist solely on tissues of the mature seed of* Dioclea megacarpa, *which contains more than 8 percent L-canavanine by dry weight. The arginyl-tRNA synthetase of the bruchid beetle larvae discriminates between L-arginine and L-canavanine, and canavanyl proteins are not synthesized. In this way, bruchid beetle larvae avoid an adverse biochemical effect of L-canavanine.*

Host plants of some mono- and oligophagous insects contain high concentrations of toxic compounds that must be either detoxified metabolically or otherwise avoided by these feeding specialists. While our understanding of insect detoxification of certain synthetic insecticides is often quite detailed, a comparable appreciation for naturally occurring defensive compounds is lacking. This deficiency will become increasingly important as humans continue to intensify their management of agricultural systems.

Many plants synthesize and accumulate large quantities of amino acid analogs (*1, 2*) that probably function as chemical barriers to the feeding activity of phytophagous insects, rodents, and other herbivores (*2–6*). An example of such a compound is L-canavanine, $H_2N{-}C({=}NH){-}NH{-}O{-}CH_2{-}CH_2{-}CH(NH_2)CO_2H$, the naturally occurring guanidinooxy structural analog of L-arginine. This amino acid is found in high concentrations in several leguminous seeds, including tropical species of *Canavalia* and *Dioclea*, where it can represent 5 to 10 percent of the dry weight (*5, 7*). In some species, arginyl-tRNA synthetase can esterify L-canavanine to arginine transfer RNA ($tRNA^{Arg}$), and this amino acid analog is readily incorporated into the nascent polypeptide chain (*8, 9*). These canavanine-containing proteins, structurally altered, severely disrupt numerous reactions of DNA and RNA metabolism as well as protein synthesis (*9, 10*). In this report, we describe how a specialist insect deals with high concentrations of a naturally occurring toxic compound in its food.

Canavanine feeding studies with the larvae of the tobacco hornworm, *Manduca sexta* (L.) (*11*); the southern cowpea weevil, *Callosobruchus maculatus* (Fabricius) (*6*); the southern armyworm, *Prodenia eridania* (Cramer) (*4*); and the boll weevil, *Anthonomus grandis* Boheman (*12*) have demonstrated the potent insecticidal qualities of this amino acid analog. In contrast, larvae of the bru-

Table 1. Fate of [^{14}C]guanidinooxy-L-canavanine injected into *Manduca sexta* and *Caryedes brasiliensis* larvae; *N* is the number of injected larvae. Comparable data were obtained in two replications of this experiment. See text for additional details.

Organism	*N*	Radioactivity (count/min)				Radioactivity recovered as $^{14}CO_2$ (%)
		Injected	TCA precipitate	Column: NH_4OH effluent	Evolved CO_2	
Manduca sexta	5	4,442,500	166,020	158,950	156,570	3.5
Caryedes brasiliensis	33	948,750	3,510	2,475	Trace	None